Heliyon 10 (2024) e38608

Contents lists available at ScienceDirect

Heliyon

journal homepage: www.cell.com/heliyon

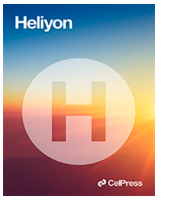

Research article

ANXA3 as a novel biomarker for sepsis diagnosis: Evidence from integrative WGCNA analysis

Jing-Xiang Zhang [a,b,1], Xin-Hao Xing [a,c,1], Ren-Yi Lu [a], Meng-Xiao Liu [a,d], Wei-Heng Xu [a], Hao-Cheng Zhang [e], Qing-Jie Zhao [a], Yan Wang [a,*]

[a] *School of Pharmacy, Second Military Medical University (Naval Medical University), Shanghai, 200433, China*
[b] *Bioinformatics Center of AMMS, Beijing, 100850, China*
[c] *International Co-operation Laboratory on Signal Transduction, Eastern Hepatobiliary Surgery Hospital, Second Military Medical University (Naval Medical University), Shanghai, 200438, China*
[d] *School of Pharmacy, Fujian University of Traditional Chinese Medicine, Fuzhou, 350108, China*
[e] *Department of Infectious Diseases, Huashan Hospital, Fudan University, Shanghai, 200040, China*

ARTICLE INFO

Keywords:
Sepsis
Biomarker
ANXA3
Bioinformatic analysis
Weighted gene Co-Expression network analysis (WGCNA)

ABSTRACT

Sepsis is a dysregulated immune response to infection that comes with multiple organ dysfunction and high mortality. The management of sepsis relies heavily on early recognition and diagnosis, but current diagnostic methods have limitations in timeliness, sensitivity, and discriminability. This study aims to discover novel biomarkers for sepsis diagnosis. Four datasets from different regions were analyzed using weighted gene co-expression network analysis (WGCNA), and genes with high Gene Significance values across these datasets were overlapped. Finally, two genes, *CD177* and *ANXA3*, were identified. *ANXA3* was validated as a potential sepsis biomarker by checking multiple datasets and Receiver Operating Characteristic (ROC) Curve Analysis. Of note, *ANXA3* could distinguish not only between adult and child sepsis patients and healthy controls, but also between septic shock and cardiogenic shock. Moreover, a murine sepsis model was established and the results showed that the transcription of *ANXA3* in peripheral blood of septic mice was significantly higher than that of healthy controls, while *Escherichia coli* infection alone did not significantly increase the transcription level of this gene. Subsequent studies of sepsis in mice revealed that the predictive effect of *Anxa3* on sepsis could be observed as early as 6 h post-modeling. Interestingly, ANXA3 expression was predominantly up-regulated in myeloid cells, up-regulated in spleen, down-regulated in lung, and not detected in liver after sepsis modeling. Taken together, this study provides a way for the discovery of biomarkers and finds that *ANXA3* may be a novel diagnostic biomarker for sepsis.

1. Introduction

Sepsis is defined as multiple organ dysfunction due to a dysregulated immune response to infection with potentially fatal results [1]. It is one of the leading causes of death worldwide and was listed as a global health priority by the World Health Organization in

* Corresponding author. School of Pharmacy, Second Military Medical University (Naval Medical University), 325 Guohe Road, Shanghai, 200433, China.
E-mail addresses: 1041474170@qq.com (J.-X. Zhang), wangyancn@smmu.edu.cn (Y. Wang).
[1] These authors contributed equally to this work.

https://doi.org/10.1016/j.heliyon.2024.e38608
Received 2 February 2024; Received in revised form 26 September 2024; Accepted 26 September 2024
Available online 30 September 2024

2017 [2]. According to a meta-analysis of 45 studies from 18 developed countries, there were 288 (95 % CI, 215–386) cases of sepsis per 100,000 people per year [3]. From 2006 to 2016, there were cumulatively 31.5 million cases of sepsis and 19.4 million cases of severe sepsis worldwide [3]. Another meta-analysis of 170 studies covering 371,937 patients reported a mean 30-day mortality rate of 24.4 % (95 % CI 21.5–27.2 %) and a mean 90-day mortality rate of 32.2 % (95 % CI 27.0–37.5 %) for sepsis [4]. Therefore, sepsis remains a serious public health problem and greatly threatens the quality of life and survival of hospitalized patients.

In 2016, at the 45th Annual Meeting of Critical Care Medicine, the American Society of Critical Care Medicine (SCCM) and the European Society of Critical Care Medicine (ESICM) jointly issued the definition and diagnostic criteria for Sepsis 3.0. The definition of Sepsis 3.0 focuses on organ dysfunction and introduces the retrospective diagnostic criteria of Sequential Organ Failure Assessment (SOFA) and quick Sequential Organ Failure Assessment (qSOFA). However, over the years, the use of SOFA and qSOFA standards has been called into question due to the delays in diagnosis and treatment they might cause [5]. Moreover, only 48 % of SOFA scores were fully in agreement with gold standard assessment, indicating the unreliability of this criteria [6]. Due to the poor sensitivity and specificity of existing biomarkers, such as C-reactive protein (CRP) and procalcitonin (PCT), researchers are also working to find new biomarkers to facilitate rapid clinical diagnosis and risk prediction [7]. More specifically, the diagnostic sensitivity of CRP for sepsis is 0.75 (95 % confidence interval [CI], 0.69–0.79), and the corresponding specificity is 0.67 (95 % CI, 0.58–0.74) [8]. As for PCT, the sensitivity is 0.77 and the specificity is 0.79 (95 % CI, 0.72–0.81 and 0.74–0.81) [8]. The sensitivity and specificity of CRP and PCT are not satisfactory.

Bioinformatic methods can provide clues for discovering novel biomarkers. In the past few decades, whole-genome analyses such as high-throughput sequencing and microarray have been widely used in the study of gene expression patterns, and massive data were generated in these processes. This has led to the development of new data analysis methods and algorithms, such as Weighted Gene Co-expression Network Analysis (WGCNA) [9], which has proven to be an effective method for biomarker discovery [10,11].

In this study, we used the WGCNA algorithm to analyze gene expression profiles of datasets from different regions. *ANXA3* was finally identified and further validated as a potential biomarker. In the context of extensive research on sepsis biomarkers worldwide [12], *ANXA3*'s significance as a marker for the clinical management of sepsis goes beyond mere diagnostic enhancement. Its capacity to discriminate septic shock from cardiogenic shock introduces a new dimension to sepsis diagnosis, promising to streamline therapeutic interventions and improve patient outcomes. Unlike conventional biomarkers that primarily reflect inflammation or organ dysfunction in a nonspecific manner, *ANXA3*'s distinct expression pattern in myeloid cells implicates its involvement in the intricate immunological responses underlying sepsis pathology. This mechanism insight not only strengthens its credibility in diagnosis but also paves a way for targeted therapeutic strategies aimed at modulating ANXA3-related pathways.

2. Materials and methods

2.1. Data collection

Datasets of gene expression profiles GSE8121, GSE13015, GSE26378, GSE26440, GSE28750, GSE57065, GSE60424, GSE65682, GSE95233, GSE131411, GSE131761, GSE134347, GSE145227, GSE154918 and GSE167363 were downloaded from the NCBI Gene Expression Omnibus (GEO) Datasets (https://www.ncbi.nlm.nih.gov/gds/). The details of the datasets were shown. (Table 1).

2.2. Construction of weighted correlation network and detection of co-expression modules

Weighted Gene Co-expression Network Analysis (WGCNA) is an R package that can build a gene co-expression network from large

Table 1
The details of the datasets used in this study.

Dataset ID	Method	Platform	Number of sepsis samples	Number of healthy control samples	Remarks
Peripheral Blood of Sepsis Patients vs. Healthy Controls					
GSE8121	Microarray	GPL570	60	15	Pediatric
GSE13015	Microarray	GPL6106	29	5	
GSE26378	Microarray	GPL570	82	21	Pediatric
GSE26440	Microarray	GPL570	98	32	Pediatric
GSE28750	Microarray	GPL570	10	20	
GSE57065	Microarray	GPL570	26	20	
GSE60424	RNA Sequencing	GPL15456	3	4	
GSE65682	Microarray	GPL13667	51	42	
GSE95233	Microarray	GPL570	51	22	
GSE134347	Microarray	GPL17586	156	83	
GSE145227	Microarray	GPL23178	10	12	Pediatric
GSE154918	RNA Sequencing	GPL20301	39	40	
GSE167363	Single cell RNA Sequencing	GPL24676	10	2	
Peripheral Blood of Sepsis Patients vs. Control Patients					
GSE131761	Microarray	GPL13497	81	15	
Peripheral Blood of Septic Shock Patients vs. Non-septic Shock Patients					
GSE131411	RNA Sequencing	GPL10999 GPL16791	63	33	

amounts of genes and identify co-expression modules [9]. The WGCNA algorithm was used to analyze the gene expression matrices of GSE28750, GSE57065, GSE134347, and GSE65682. The samples were first clustered according to the gene expression profiles to eliminate the outliers. The network was then made to correspond to the power-law distribution that simulated the actual biological network state by setting a soft threshold [13]. To group genes with similar expression patterns, the scale-free network was lastly built using the "blockwiseModules" function, then the module partitioning analysis was performed to discover gene co-expression modules based on the topological overlap.

2.3. Identification of clinically related genes

The foremost principal component of each module was calculated as a synthetic gene (Module eigengene, ME), representing the expression profiles of all genes in this module [14]. Next, the correlation between MEs and clinical traits (diagnosed with sepsis or healthy) for all modules was calculated. Then, to determine which genes are most correlated with sepsis, the gene-trait significance (GS) value was calculated by Person's correlation for each gene in each dataset, and the common genes with high values were finally found across the four datasets using Venn's diagrams on Venny 2.1 (https://bioinfogp.cnb.csic.es/tools/venny/index.html).

2.4. Receiver Operating Characteristic (ROC) Curve Analysis

ROC curves were plotted for 9 datasets including GSE95233, GSE154918, GSE13015, GSE60424, GSE131761, GSE8121, GSE26378, GSE26440, and GSE145227. The R package "pROC" was used to evaluate the performance of the biomarkers based on specificity and sensitivity. Moreover, the area under curve (AUC) values were calculated for selected genes to assess their diagnostic potential as biomarkers.

2.5. Single-cell RNA-seq analysis

The single-cell RNA sequencing dataset GSE167363 on the GEO platform were used for analysis. After downloading the Raw Count matrix of this dataset, sample integration, quality control, and re-clustering were performed. The Harmony method was used to correct for batch effects and the Seurat package were used for data normalization, dimensionality reduction, and clustering. Subsequently, each cluster were annotated based on reference marker genes of cell types.

2.6. Animals

Female C57BL/6 mice (6–8 weeks old), weighing 18–22 g, were purchased from the SLAC Laboratory Animal Company (Shanghai, China) and used in all experiments. The rearing humidity of mice was about 55 %, and the temperature was 20–22 °C. Mice were given free access to food and water. Moreover, light or dark environments were given according to their circadian rhythm.

2.7. Cecal ligation and puncture (CLP)-Induced sepsis

The poly-microbial sepsis was induced by CLP as previously described [15]. Briefly, the mice were anesthetized by intraperitoneal injection of sodium pentobarbital solution. The concentration of the sodium pentobarbital solution is 0.5 %, and the dosage is 100 injections per 10g body weight intraperitoneally. Hair on the surgical area was removed with Veet® Depilatory Cream (Reckitt Benckiser, Beijing, China) and the area was cleaned and disinfected by alcohol cotton balls. A midline incision was made to obtain access to the cecum, which was then exposed, ligated, and punctured with a 22-gauge needle. The location of the ligation is at the midpoint of the cecum. The cecum was put back in place before the incision was closed. The peritoneum and skin were sutured separately. Povidone-iodine was used for post-operative disinfection. After these steps, the mouse was immediately resuscitated by normal saline at 37 °C (1 ml in total per 20 g body weight) subcutaneously at the root of both thighs. Besides, appropriate measures were taken to alleviate the pain of mice. All mice were covered with cotton for warmth after surgery. Sham-operated animals underwent anaesthetization, incision, exposure, and suture, but without cecal ligation and puncture. After 6,12, or 24 h of CLP or sham operation, the peripheral blood of each mouse was collected using heparin sodium anticoagulant tubes. The sample size of each group was 4.

2.8. Escherichia coli-induced infection

The *Escherichia coli* (*E. coli*)-induced intra-abdominal infection was induced by injection as previously described [16]. Briefly, the mice were infected by intraperitoneal injection of 1×10^7 CFU of *E. coli* strain DH5α in 0.2 mL of PBS. After 24 h of infection, the peripheral blood of each mouse was collected as described above.

2.9. RNA Extraction, reverse transcription, and quantitative real-time PCR

The Red Blood Cell Lysis Buffer (Biosharp, Hefei, China) was used to prepare suspensions of white blood cells from peripheral blood for subsequent experiments. Total RNA was extracted using the RNA Fast 200 Kit (Fastagen, Shanghai, China). Then the Hifair® III 1st Strand cDNA Synthesis SuperMix (Yeasen, Shanghai, China) was used for reverse transcription. Quantitative real-time PCR was

conducted with the Hieff® qPCR SYBR Green Master Mix (Yeasen, Shanghai, China) and StepOnePlus Real-Time PCR System (Thermo Scientific, Massachusetts, United States). It is worth noting that before starting the machine, the sealing film must be tightly covered to maintain sealing. All experimental procedures were performed following the manufacturer's recommendations. The *Gapdh* gene was used as an endogenous reference. Specific amplification was ensured by observing the dissolution curves. The primer sequences of *Anxa3* and *Gapdh* were as follows. *Anxa3*: forward GACTTGGGACTGACGAGAAAAC; reverse CCACCATGACGTGCTCGAA. *Gapdh*: forward TCACCATCTTCCAGGAGCGAGAC; reverse AGACACCAGTAGACTCCACGACATAC.

2.10. Immunohistochemistry

Mouse organs were harvested and sectioned 24 h after the sepsis modeling. Then the tissue sections were deparaffinized with Xylene for 3 times, and rehydrated with gradient ethanol, and antigen retrieval was performed by heating the tissue sections in 0.01 M (pH 6.0) citrate buffer in a microwave oven. 3 % H_2O_2 was then used for blocking endogenous peroxidase. Next, the ANXA3 primary antibody (AF5159, Affinity Biosciences, Shanghai, China, 1:100 dilution) was dropped into the sections, and they were incubated overnight at 4 °C. After three times of washing, the HRP-conjugated secondary antibody (S0001, Affinity Biosciences, Shanghai, China, 1:200 dilution) was added and incubated at 25 °C for 60 min, followed by diaminobenzidine (DAB) staining. Then hematoxylin (Beyotime Biotechnology, Shanghai, China) was used for counterstaining and inverted microscopes were used to take pictures for these sections.

2.11. Flow cytometry

The spleen, thymus, peripheral blood, and peritoneal lavage fluid of the mice were collected 24 h after the sepsis modeling. The spleen and thymus were ground into single-cell suspensions. For the peripheral blood and spleen, red blood cells were lysed as described above.

The cells were washed with phosphate buffer saline (PBS) containing 5 % fetal bovine serum. Then the Fc receptors on the cells were blocked for 15 min by the Purified Rat Anti-Mouse CD16/CD32 antibody (Catalog No:553142, BD Biosciences, New Jersey, US, 1:25 dilution). The cells were next resuspended in 200 μL of PBS and antibodies were added according to their instructions. Then, cells were collected, washed with PBS containing 5 % fetal bovine serum, and collected for testing. For secondary antibody staining, the cells were incubated with secondary antibodies for 1 h, then they were collected and washed with PBS containing 5 % fetal bovine serum before testing.

The sources of antibodies were as follows: BV421-conjugated anti-mouse CD19 antibody (Catalog No: A14905, 1:250 dilution), APC-conjugated anti-mouse CD3 antibody(Catalog No: 17-0032-82, 1:250 dilution), PE-conjugated anti-mouse Ly6G antibody (Catalog No: 12-9668-82, 1:250 dilution), FITC-conjugated anti-mouse CD11b antibody (Catalog No: 11-0112-82, 1:250 dilution) and FITC-conjugated anti-mouse F4/80 antibody (Catalog No: 11-4801-82, 1:250 dilution) were purchased from Thermo Fisher Scientific, Massachusetts, US. Rabbit-anti-mouse ANXA3 primary antibody (Catalog No: AF5159, 1:100 dilution), Alexa Fluor 488-conjugated anti-rabbit secondary antibody (Catalog No: S0018, 1:133 dilution), Alexa Fluor 594-conjugated anti-rabbit secondary antibody

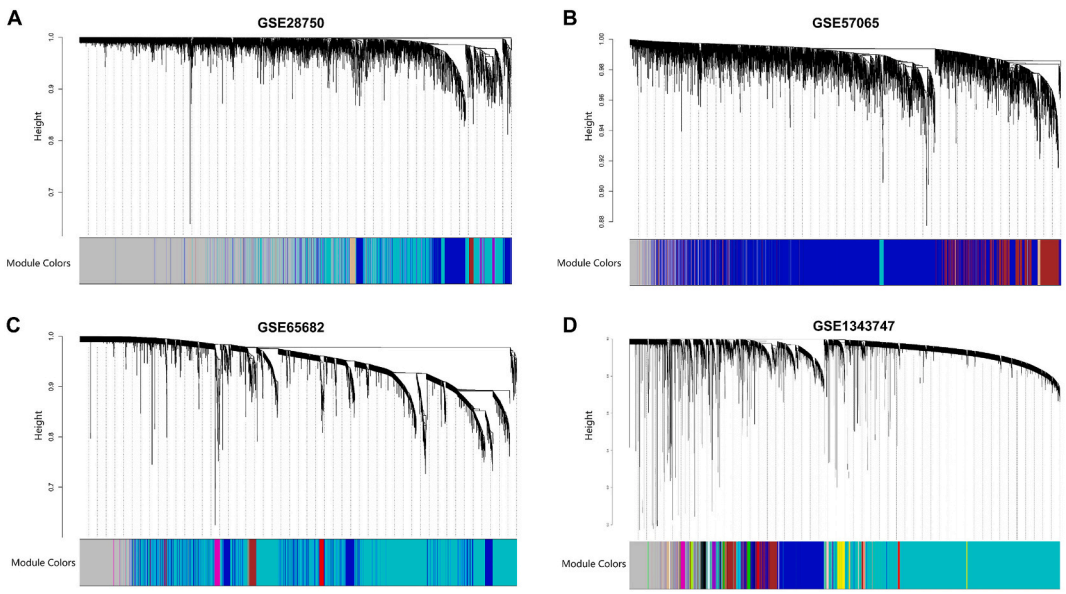

Fig. 1. Clustering dendrograms of genes, based on the topological overlap, together with assigned module colors for the four datasets using the WGCNA algorithm. For each dataset, modules were constructed and were shown in different colors. WGCNA: Weighted Gene Co-expression Network Analysis.

(Catalog No: S0006, 1:133 dilution) and Alexa Fluor 647-conjugated anti-rabbit secondary antibody (Catalog No: S0013, 1:133 dilution) were purchased from Affinity Biosciences, Shanghai, China.

2.12. Data analysis

Data of quantitative real-time PCR was processed by 2^(–delta delta Ct) method [17]. The immunohistochemistry results were processed using ImageJ software. The flow cytometry results were processed using FlowJo software. Then these data were analyzed and plotted using GraphPad Prism. After confirming the normality distribution and homogeneity of variance, unpaired t-tests were performed. *P < 0.05, **P < 0.01, ***P < 0.001.

3. Results

3.1. Weighted gene Co-expression network analysis (WGCNA) and screening for clinically related modules and genes

The NCBI GEO database was utilized to obtain gene expression profile datasets in the peripheral blood of septic patients. Four datasets (GSE28750, GSE57065, GSE65682, and GSE134347) representing different populations from France, the United States, the Netherlands, and Malta were obtained from the GEO database. Gene expression matrices of these four datasets were analyzed by the WGCNA R package. Gene modules, representing groups of genes with similar patterns of expression, were calculated for each dataset. Moreover, the hierarchical clustering dendrogram for each dataset was plotted and each module was assigned a unique color (Fig. 1A–D). These dendrograms and modules reflected the co-expression status of genes in the whole blood of patients, which may have potential values for revealing the pathological mechanisms of sepsis.

Gene Significance (GS) is defined as the absolute value of the Pearson correlation coefficient between a gene and the clinical diagnosis in the WGCNA algorithm, which was used to quantify the correlation between them. GS values of all genes in the 4 datasets were calculated to evaluate the correlation between each gene and sepsis diagnosis. The top 15 genes with the highest values were selected in each dataset (Table 2). The top 15 genes in GSE28750 included *MCEMP1*, *S100A12*, *RETN*, *PLBD1*, *S100A9*, *HP*, *CYSTM1*, *CD177*, *ANXA3*, *CLEC4D*, *TLR5*, *GPR84*, *MS4A6A*, *RAB13*, and *USB1*. The top 15 genes in GSE57065 included *IRAK3*, *MCEMP1*, *TLR5*, *ANXA3*, *S100A9*, *SLC26A8*, *GRB10*, *PLBD1*, *RNASE2*, *FCAR*, *CD177*, *PGS1*, *GYG1*, *AGTRAP*, and *BCL6*. The top 15 genes in GSE65682 included *C19orf59*, *CD177*, *GADD45A*, *ARG1*, *CLEC4D*, *C5orf32*, *GYG1*, *HK3*, *UPP1*, *RGL4*, *ANXA3*, *SERPINB1*, *IRAK3*, *FCAR*, and *GPR84*. The top 15 genes in GSE134347 included *C19orf59*, *ANXA3*, *S100A8*, *S100A9*, *CD177P1*, *GYG1*, *CD177*, *MAPK14*, *CLEC4D*,

Table 2
The top 15 genes with the highest GS values for GSE28750, GSE57065, GSE65682, and GSE134347 were analyzed by WGCNA.

Dataset ID	Gene Name	GS Value	Gene Name	GS Value
GSE28750	*MCEMP1*	0.961131	*ANXA3*	0.9147
	S100A12	0.946505	*CLEC4D*	0.91292
	RETN	0.932495	*TLR5*	0.912155
	PLBD1	0.931995	*GPR84*	0.911295
	S100A9	0.930776	*MS4A6A*	0.909924
	HP	0.926046	*RAB13*	0.908034
	CYSTM1	0.917831	*USB1*	0.908929
	CD177	0.915821		
GSE57065	*IRAK3*	0.941714	*RNASE2*	0.900972
	MCEMP1	0.940526	*FCAR*	0.900401
	TLR5	0.929993	*CD177*	0.89784
	ANXA3	0.922709	*PGS1*	0.897277
	S100A9	0.909233	*GYG1*	0.896734
	SLC26A8	0.906817	*AGTRAP*	0.895421
	GRB10	0.903617	*BCL6*	0.893732
	PLBD1	0.902745		
GSE65682	*C19orf59*	0.977931	*UPP1*	0.962505
	CD177	0.969728	*RGL4*	0.959306
	GADD45A	0.969718	*ANXA3*	0.958931
	ARG1	0.96606	*SERPINB1*	0.957891
	CLEC4D	0.965557	*IRAK3*	0.95718
	C5orf32	0.963431	*FCAR*	0.956853
	GYG1	0.963403	*GPR84*	0.954416
	HK3	0.963181		
GSE134347	*C19orf59*	0.94364	*CLEC4D*	0.901065
	ANXA3	0.925584	*HMGB2*	0.900694
	S100A8	0.918015	*IRAK3*	0.897906
	S100A9	0.917185	*CR1L*	0.895963
	CD177P1	0.912387	*TLR5*	0.895031
	GYG1	0.90751	*ARG1*	0.893785
	CD177	0.902363	*METTL9*	0.892966
	MAPK14	0.901566		

HMGB2, *IRAK3*, *CR1L*, *TLR5*, *ARG1*, and *METTL9*.

Next, the overlapped genes in the four results were found using Venn's diagram. It can be seen that there were two genes, *ANXA3* and *CD177*, shared by the four results (Fig. 2), indicating that these genes were highly correlated with the clinical phenotype of sepsis, regardless of geographical location or genetic background.

3.2. *ANXA3* expression is sharply up-regulated in blood samples of septic patients

CD177 had been reported as a biomarker of sepsis previously [18,19], while it is verified to be a biomarker only in lung tissue experimentally [18]. Therefore, we focused our attention on whether the other gene, *ANXA3*, could act as a sepsis biomarker. More datasets were used for validation *in silico*. As for age, 5 datasets were conducted in adults and 4 in pediatric subjects. As for geographical locations or ethnicities, 5 were from North America, 3 from Europe, and 1 from Asia. As for experimental settings, 7 were performed using microarray and 2 using RNA-sequencing. Among the 9 datasets, *ANXA3* was all sharply up-regulated in the peripheral blood samples of septic patients compared with the control groups (Fig. 3), regardless of ethnicity, age, or experimental settings.

Besides, ROC curves were generated from each dataset to confirm the performance of *ANXA3* as a biomarker (Fig. 3). A good biomarker should have high sensitivity (the ability to correctly identify true positives) and specificity (the ability to correctly identify true negatives), which is reflected by the high AUC value of the ROC curve. The AUC values for *ANXA3* varied between 0.883 and 1.000, equal to or close to 1.000 in all 9 datasets, indicating that *ANXA3* has excellent diagnostic performance (Fig. 3).

3.3. *ANXA3* helps to make an accurate diagnosis of sepsis

The results of different ages, races, and experiment settings above proved that the transcription of *ANXA3* was significantly up-regulated in the peripheral blood samples of septic patients compared with healthy controls. We next studied whether this gene could distinguish sepsis from diseases with similar symptoms. The dataset GSE131411 contained peripheral blood samples from both septic shock and cardiogenic shock cases. It can be seen that the transcript level of *ANXA3* was significantly higher in the septic shock group than in the cardiogenic shock group (Fig. 4). Since septic shock is a severe form of sepsis and shares similar signs and symptoms with non-septic shock (such as cardiogenic shock), it is of great value to utilize *ANXA3* as a potential biomarker to distinguish the two conditions.

3.4. *ANXA3* exhibits stable expression across different neutrophil subpopulations

Since *ANXA3* is expressed restrictively in neutrophils in blood leukocyte populations [20], we next investigated whether different expression of *ANXA3* exists in different neutrophils subtypes in the blood of sepsis patients. The single-cell RNA sequencing dataset GSE167363 was used in this study. After downloading the data, merging samples, quality control, re-clustering, batch effect removal, standardization, dimensionality reduction, and re-clustering, all cells were divided into 13 clusters with a resolution of 0.3, and each cluster was annotated according to the reference cell type marker gene (Fig. 5A). The results showed that *ANXA3* predominantly expressed in neutrophils, although there is some low expression in other cell types. (Fig. 5B). And then we focused on the neutrophils. After removing a few misclustered monocytes and erythroid cells (Supplementary Fig. 1), the re-clustering process was performed, resulting three subpopulations of neutrophils (Fig. 5C). There were no significant differences in the expression levels of *ANXA3* among these subpopulations (Fig. 5D), indicating stable expression of this gene.

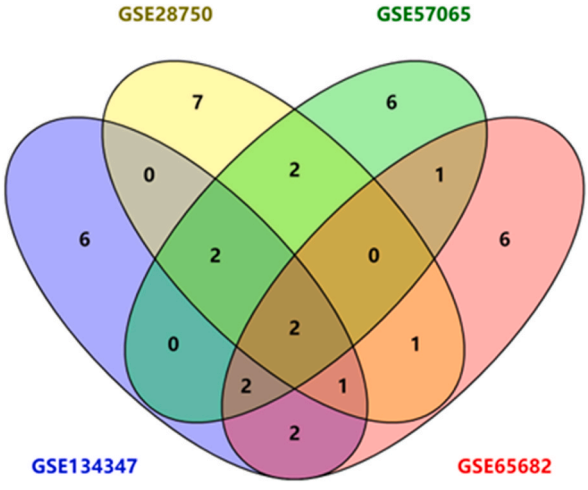

Fig. 2. The Venn diagram showed the shared significant genes of the four datasets. There were only two shared genes (*ANXA3* and *CD177*) in the four results. ANXA3: Annexin A3.

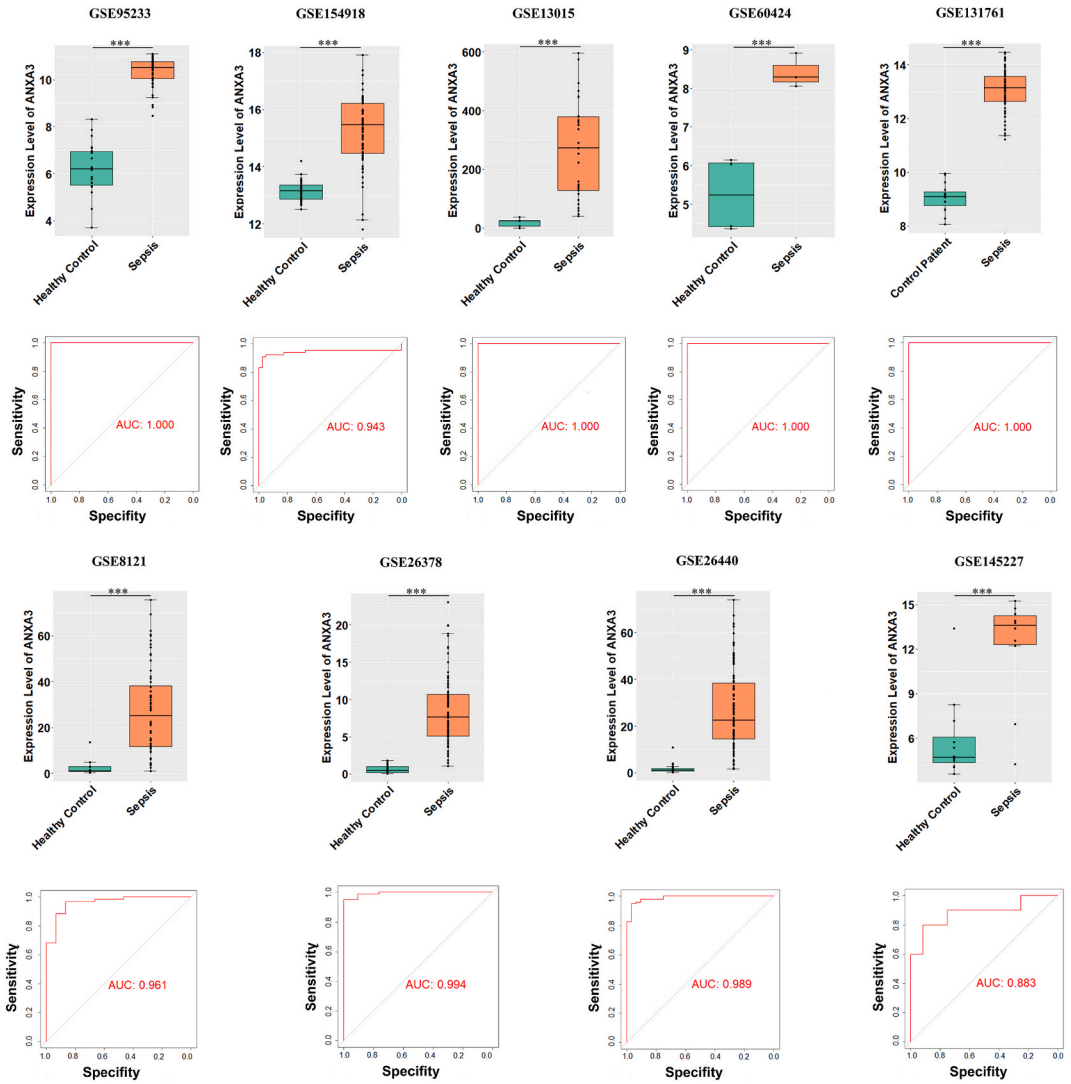

Fig. 3. The *ANXA3* gene was significantly up-regulated in sepsis patients compared to controls. Each box plot represented the expression level of *ANXA3* in peripheral blood. The first five studies were conducted in the adult groups, and the last four were conducted in the pediatric groups. The ROC curve of each dataset was located below the corresponding boxplot, and the area under the curve (AUC) was used to investigate the diagnostic value of the *ANXA3* gene as a biomarker, ***P < 0.001. ROC: Receiver Operating Characteristic. AUC: Area Under Curve.

3.5. *Validation of Anxa3 as a potential biomarker in murine sepsis model*

The above results *in silico* suggested that *ANXA3* was a good biomarker that could distinguish sepsis from healthy controls and septic shock from similar conditions. To verify the upregulation in sepsis, we established a murine sepsis model by CLP and investigated the transcript levels of *Anxa3 in vivo*. In addition, to rule out the possibility that the up-regulation of *Anxa3* was due to a simple infection, we also established an *E. coli* infection model. At 24 h after modeling, the peripheral blood of mice was collected and lysed to remove red blood cells. Total mRNA was extracted and reverse-transcribed into cDNA, and the relative transcript levels of *Anxa3* were measured by quantitative real-time PCR. The result showed that the transcription of *Anxa3* was significantly increased in the peripheral blood of septic mice (Fig. 6A) (n = 4 for each group. Unpaired t-tests were performed. **P < 0.01.), demonstrating the potential of *Anxa3* as a biomarker. Moreover, *E. coli* infection did not significantly increase *Anxa3* transcription (Fig. 6A). This suggests that the up-regulation of *Anxa3* is specific in sepsis, and that other factors rather than just infection may be responsible for this biomarker effect. In addition, to verify whether *Anxa3* can serve as an early biomarker for sepsis, we detected the expression levels of *Anxa3* in the whole blood of septic mice at 6 h, 12 h, and 24 h post CLP. The results showed that the expression level of *Anxa3* was significantly up-regulated as early as 6 h after sepsis modelling (Fig. 6B). This suggests the predictive value of *ANXA3* for early-stage sepsis.

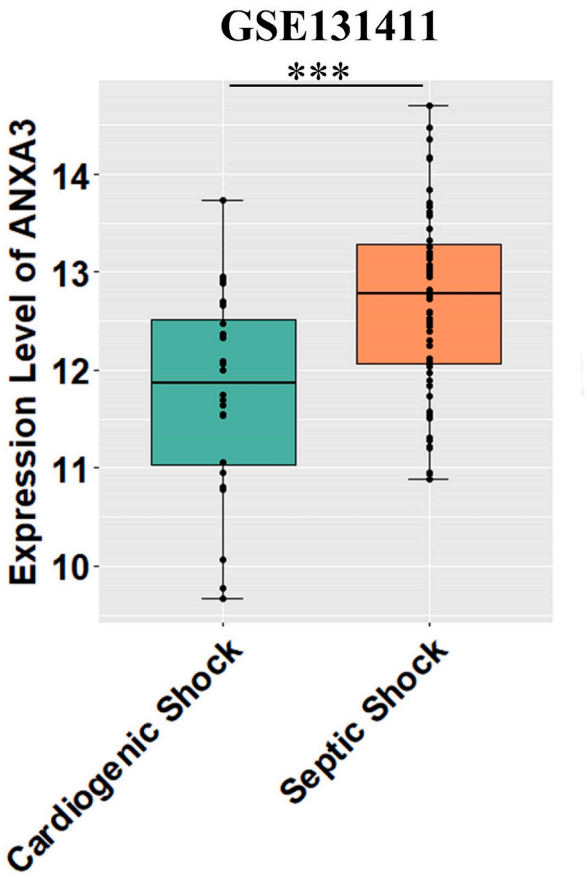

Fig. 4. *ANXA3* could help to distinguish septic shock from cardiogenic shock. The dataset GSE131411 from Spain showed that the expression of *ANXA3* was significantly higher in peripheral blood samples of septic shock patients compared to cardiogenic shock. ***P < 0.001.

3.6. *ANXA3 was up-regulated in the myeloid cells in septic mice*

The expression of a certain protein on particular cell populations can indicate a certain pathological state. For example, an upregulation of Pentraxin-3 (PTX3) in dendritic cells and macrophages reflects a hyperinflammatory state of sepsis [21], and a decreased monocytic human leukocyte antigen DR (mHLA-DR) represents a later immunosuppressive state [22]. To explore the expression of ANXA3 on particular types of immune cells during sepsis comprehensively, we established the mouse sepsis model as described above and harvested the peripheral blood, peritoneal lavage, spleen, and thymus 24 h after CLP. Since *ANXA3* shows restricted expression to neutrophils among blood leukocyte populations [20], blood neutrophils were first stained and analyzed by flow cytometry. The results showed that the proportion of $ANXA3^+$ cells in blood neutrophils ($Ly6G^+$) was significantly increased (Fig. 7A) (n = 4 for each group. Unpaired t-tests were performed. *P < 0.05, **P < 0.01, ***P < 0.001.). Then, other primary myeloid cells (including total myeloid cells in the peritoneal cavity, peritoneal cavity neutrophils, and peritoneal cavity macrophages) and primary lymphoid cells (including spleen B cells, thymic T cells) were also collected, stained, and analyzed by flow cytometry. The results showed that the proportions of $ANXA3^+$ cells were significantly increased in peritoneal macrophages ($F4/80^+$), neutrophils ($Ly6G^+$), and total myeloid cells ($CD11b^+$) after CLP (Fig. 7B–D). Moreover, the ratio of $ANXA3^+$ spleen B cells ($CD19^+$) also showed an increasing trend in septic mice (Fig. 7E). Of note, there was no $ANXA3^+$ thymic T cells ($CD3^+$) detectable in either sham-operated or septic mice (Fig. 7F), consistent with previous reports [20]. Collectively, ANXA3 was up-regulated mainly in the myeloid cells after sepsis modeling.

3.7. *ANXA3 protein was up-regulated in the spleen, down-regulated in the lung, and was not detected in the liver of septic mouse*

Since *CD177* had been reported as a biomarker of sepsis only in lung tissue experimentally, we further investigated the expression of ANXA3 protein in the spleen, lung, and liver. Organs were harvested 24 h after CLP, and immunohistochemistry was performed. The results showed that sepsis modeling could lead to a significant increase in the protein level of ANXA3 in the spleen compared with the sham-operated group (Fig. 8A). The immunohistochemical results of the lung sections showed that ANXA3 in the vascular endothelium was significantly down-regulated in septic mice (Fig. 8B). As shown in the figure, ANXA3 is expressed in vascular endothelial cells,

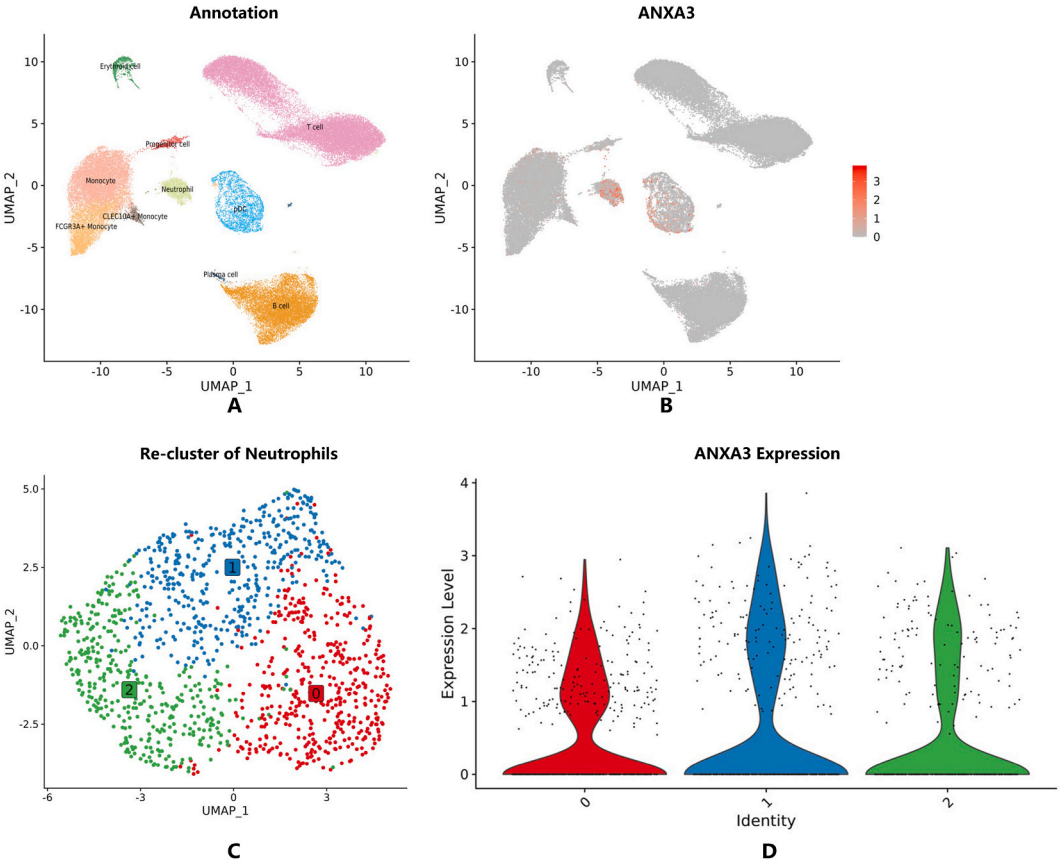

Fig. 5. Stability of *ANXA3* expression across different neutrophil subpopulations. (A) Cellular heterogeneity revealed by clustering analysis, with all cells segregated into 13 distinct clusters at a resolution setting of 0.3. (B) *ANXA3* is highly expressed in neutrophils, while showing minimal expression in other cell types. (C) Illustration of the three identified neutrophil subpopulations. (D) Quantitative analysis confirms no significant difference of *ANXA3* expression levels across the three neutrophil subsets, indicating consistent expression profiles.

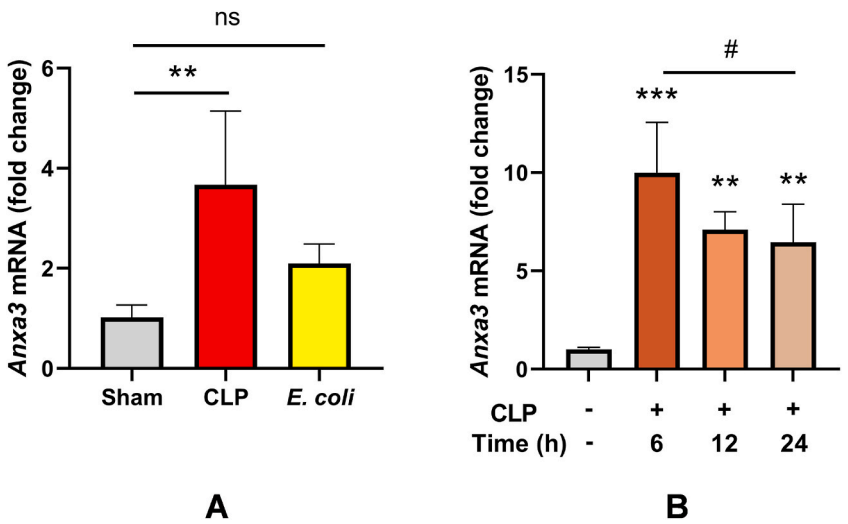

Fig. 6. Validation of *Anxa3* as a biomarker of sepsis in mice. (**A**) Quantitative real-time PCR illustrating the significant upregulation of *Anxa3* in the peripheral blood of mice after CLP modelling, but not in simple *E. coli* infection. Transcript abundance of *Anxa3* in the peripheral blood were measured at 24 h after modelling. n = 4 for each group. **P < 0.01. (B) The expression level of *Anxa3* was significantly up-regulated as early as 6 h post CLP, suggesting that *Anxa3* has predictive value in early sepsis. PCR: Polymerase Chain Reaction. CLP: Cecal Ligation and Puncture. *E. coli: Escherichia coli*.

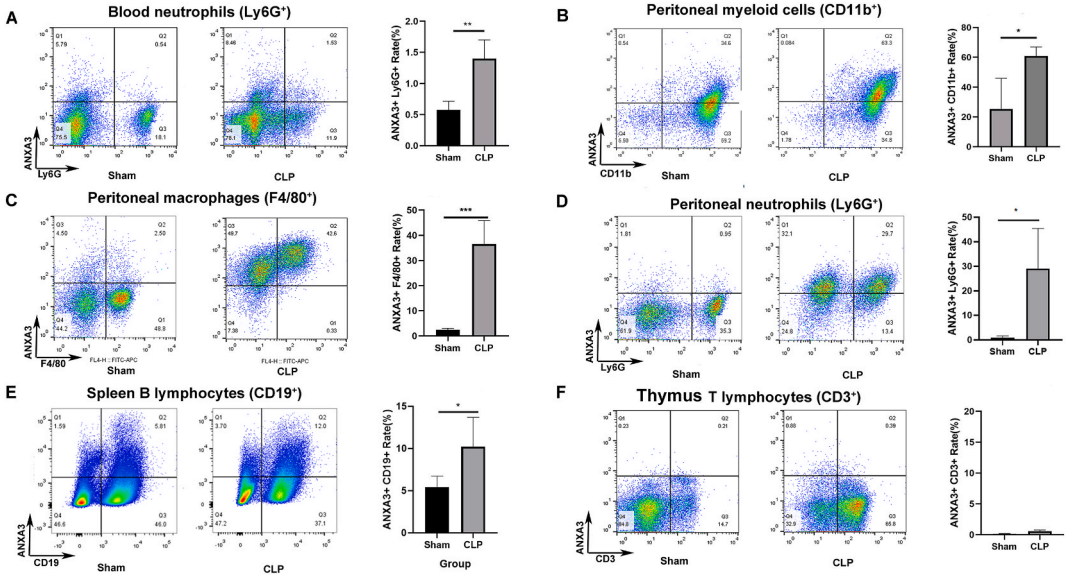

Fig. 7. Positive ratios of ANXA3 protein in immune cells in septic mice as measured by flow cytometry. (**A**) blood neutrophils (gated as $Ly6G^+$); (**B**) peritoneal myeloid cells (gated as $CD11b^+$); (**C**) peritoneal macrophages (gated as $F4/80^+$); (**D**) peritoneal neutrophils (gated as $Ly6G^+$); (**E**) spleen B cells (gated as $CD19^+$); (**F**) thymus T cells (gated as $CD3^+$). n = 4 for each group. *P < 0.05, **P < 0.01, ***P < 0.001. CLP: Cecal Ligation and Puncture.

indicating it may have certain functions in these cells, which warrant further investigation. In the liver, ANXA3 protein was rarely detected, and it did not show a significant change after sepsis modeling (Fig. 8C).

4. Discussion

Early recognition of sepsis is a prerequisite for appropriate treatment to reduce organ system damage and mortality. SOFA is

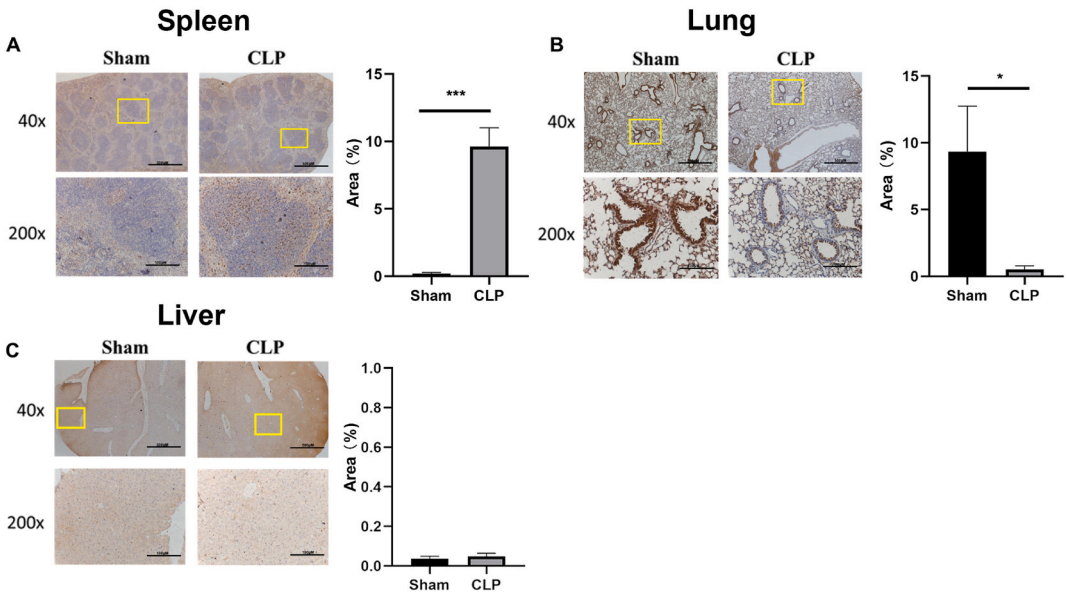

Fig. 8. The expression level of ANXA3 protein in the spleen (**A**), lung (**B**), and liver (**C**) in septic mice. After 24 h after CLP, the organs were harvested, and abundances of ANXA3 protein were evaluated and quantitated by immunohistochemical staining. ANXA3 was significantly up-regulated in the spleen (**A**) and significantly down-regulated in the pulmonary vascular endothelium (**B**) in septic mice. Also, this protein showed few abundances in the liver (**C**). The CLP operation was utilized to induce sepsis. n = 3 for each group. *P < 0.05, ***P < 0.001. In 40 × magnification and 200 × magnification, the scale bar represents 500 μm and 100 μm respectively. CLP: Cecal Ligation and Puncture.

currently the gold standard for sepsis diagnosis based on multi-organ dysfunction [1]. However, SOFA and qSOFA are retrospective and based on global organ function which lacks diagnostic specificity. The pathogenesis and development of sepsis are very complex, so it relies on molecular biomarkers to indicate different aspects of sepsis. For example, CRP, PCT, and IL-6 indicate infection or inflammation, thrombomodulin indicates coagulation, lactate indicates tissue hypoxia, angiopoietin-2 indicates endothelial injury, and mHLA-DR indicates immunosuppression [23]. Regrettably, these biomarkers lack the accuracy and specificity to accurately diagnose sepsis early. This may be the reason why the success of CLP modeling does not depend on these biomarker indications [15]. Collectively, sepsis requires more effective biomarkers.

Traditionally, searching for genes most related to diseases between patients and healthy people was the starting point for biomarker discovery. Blood-derived biomarkers are more applicable in clinical practice since the peripheral blood of patients is relatively easier to obtain than tissue sections. In the past decades, the widespread application of whole-genome technologies and bioinformatics analysis methods have made it possible to find significant genes on a large scale and provided a new way to discover biomarkers in blood [24]. In this study, four datasets from different regions were first analyzed using the WGCNA bioinformatics algorithm. The results showed that *ANXA3* and *CD177* were the overlapped genes shared by the datasets of different races. Considering that *CD177* expression had been proved not up-regulated in peripheral blood but in lung tissue in response to sepsis modeling, and lung tissue is clinically difficult to obtain [18], the unstudied gene *ANXA3* was selected for further research. The results showed that the transcript abundance of *ANXA3* in the whole blood of patients with sepsis was higher than that of healthy controls, and this gene was more highly expressed in septic shock which could distinguish septic shock from cardiogenic shock. A good biomarker should demonstrate both high sensitivity and specificity. The ROC curve describes the relationship between the sensitivity and specificity of a biomarker with different cutoff values. In all datasets, the AUC values of *ANXA3* were equal to or close to 1, suggesting that *ANXA3* has the potential to be a biomarker of sepsis. Of note, we found that *ANXA3* has the potential to act as a biomarker alone in both adults and children, expanding on previous findings [25]. In addition, when we reviewed the literature, we did not find any non-specific inflammatory biomarkers, such as PCT and CRP, that could distinguish between septic shock and cardiogenic shock, whereas *ANXA3* could.

We screened *ANXA3* and preliminarily validated its performance as a biomarker *in silico*. Further, its performance was verified by murine experiments. The results of quantitative real-time PCR indicated that the expression of *Anxa3* was significantly increased in blood samples from septic mice, while this effect was not present in mice with simple infection. This demonstrated the performance of *Anxa3* as the blood biomarker for sepsis in mice.

There is no evidence that ANXA3 is a secreted protein, so it cannot be detected at the extracellular level, and detection at the intracellular level may result in high detection costs [26]. Our study identified the biomarker potential of *ANXA3* at the transcriptional level, enabling it to diagnose sepsis with a fast and simple qPCR. Given that whole blood can be obtained quickly and easily, the use of the transcription level of *ANXA3* in the diagnosis of sepsis may have broad application prospects.

In addition, the expression changes of ANXA3 in different tissues and immune cells were studied for the first time by immunohistochemistry and flow cytometry, providing a landscape for its pathological expression pattern and clues to the potential function of ANXA3 in sepsis. Previous studies reported that ANXA3 was mainly expressed on neutrophils under normal conditions [20]. In this study, we further revealed that the expression of ANXA3 was significantly increased in myeloid cells in sepsis (Fig. 7). Myeloid cells constitute more than half of the leukocytes in the whole blood and are even higher in sepsis. Therefore, using *ANXA3* as a biomarker has an advantage in blood sample tests in clinical practice.

ANXA3 is a member of the annexin family, and its length is 323 amino acids, with 4 conserved domains, 5 α helices, and a Ca^{2+} binding site [20,27–29]. The annexin family is a structurally homologous Ca^{2+}-dependent phospholipid-binding protein, which has omnifarious functions, including maintaining the integrity of the cytoskeleton and extracellular matrix, affecting endocytosis and exocytosis, regulating ion channel transport, participating in membrane fusion and extracellular secretion, and regulating cell proliferation, differentiation, and apoptosis [30–36]. ANXA3, in particular, is associated with the vesicle transport, cell membrane fusion, and cell granule aggregation in neutrophils, which may contribute to pathogen clearance and infection resolution in sepsis on one hand, but exacerbating inflammation and organ damage on the other hand [37,38]. Overexpression of ANXA3 enhanced the proliferation and migration of microglia [39], while these behaviors of myeloid cells, if any, in sepsis may contribute to pathogen clearance or exacerbate the inflammatory cascade. Since numerous immune cells underwent apoptosis in the spleen during sepsis [40], the up-regulated expression of ANXA3 in the spleen may be a response to immune cells' proliferation and migration (Fig. 8A). Among the multiple organ dysfunctions in sepsis, lung injury was the earliest and most common, and vascular endothelial injury was an important component of lung injury [41]. The down-regulated expression of ANXA3 in the vascular endothelium suggested that it might be associated with pulmonary vascular endothelial injury (Fig. 8B). Moreover, as sepsis initially presents as a state of hyperactive immunity, which subsequently transitions into immunosuppression. Considering that decreased ANXA3 expression might contribute to the suppression of excessive inflammatory responses [42], the downregulation of ANXA3 in the lung might be a manifestation of pulmonary immunosuppressive state. Collectively, the role of ANXA3 in sepsis is still unclear and worth further exploring. Since ANXA3 expression is mainly elevated in myeloid cells upon sepsis, we are planning to construct transgenic mice harboring a conditional deletion of ANXA3 in myeloid cells to investigate its role in the myeloid system comprehensively in sepsis.

Compared with traditional sepsis biomarkers, *ANXA3* has the following advantages: First, the sample acquisition is straightforward and peripheral blood can be used as a test sample. Second, it is helpful to distinguish between cardiogenic shock and septic shock, which is helpful for clinical judgment. Third, it has good sensitivity and specificity. Therefore, the integration of *ANXA3* into existing frameworks for sepsis diagnosis has the potential to facilitate rapid diagnosis, risk prediction, and stratification.

In fact, *ANXA3* has been used as an independent or combined biomarker in other fields, such as COVID-19 [43], ischemic stroke [44], and ovarian serous carcinoma [45]. *ANXA3*'s versatility in reflecting pathological states underscores its importance in the clinical setting, where it might facilitate early detection and disease monitoring. *ANXA3* is a subject of keen interest for researchers

aiming to elucidate disease mechanisms and develop targeted therapies. Therefore, it is necessary to continue to explore the expression pattern and functional significance of *ANXA3* in a range of diseases in order to fully utilize its clinical application.

Previous studies have also shown high expression of *ANXA3* in whole blood of patients with sepsis, which is consistent with our work [20,42]. In this study, we found that *ANXA3* has the potential to act as a biomarker alone in both adults and children, and evaluated the sensitivity and specificity of the *ANXA3* gene, explored differences in its expression in sepsis versus simple infection, and investigated its potential as a distinct biomarker for sepsis.

Although the WGCNA algorithm has been used in numerous studies, it has previously been limited to building gene co-expression modules. In this study, we tried to identify genes with high GS values using various datasets, and then searched for common genes in these datasets. The value of this study lies not only in the discovery of *ANXA3* as a biomarker, but also in the discovery of a new method that can then be used to find biomarkers in other diseases. Given that GS value is calculated as the correlation coefficient between the expression level of each gene and the disease status, it is more likely to be biologically relevant [9]. This is an advantage of the new method over the traditional methods. In the future, this method has the potential to be applied to discover more biomarkers for diseases.

Nevertheless, due to the limitations of our laboratory conditions, this study did not include comparative analyses with other biomarkers (PCT, CRP, IL-6) or diagnostic criteria (SOFA, qSOFA). In addition, due to ethical issues, we did not collect blood samples from patients with clinical sepsis to verify the effects of *ANXA3* as a biomarker. Clinicians are welcome to further validate the accuracy and advantages of *ANXA3* as a diagnostic marker in future clinical work.

5. Conclusions

In this study, we revealed and confirmed that *ANXA3* is a novel biomarker of sepsis. It has a potential broad application prospect in the diagnosis of clinical sepsis.

Funding

This study was supported by the Natural Science Foundation of China (81772124 to Y.W.) and the Shanghai Science and Technology Committee (20S11902900 to Y.W. and 22YF1445800 to H.C.Z.).

Ethics approval and consent to participate

This study was approved and supervised by the Ethics Committee of Second Military Medical University (Naval Medical University), Shanghai, China, with the approval number: 81772124. All animal studies complied with the ARRIVE guidelines. Patient data were obtained from the publicly open database GEO and informed patient consent was not applicable.

Data availability

Data used to perform bioinformatic analysis are available from the NCBI Gene Expression Omnibus (GEO) databases, which can be found at https://www.ncbi.nlm.nih.gov/geo/. And the experimental data in the current study are available from the corresponding author on reasonable request.

CRediT authorship contribution statement

Jing-Xiang Zhang: Writing – original draft, Visualization, Validation, Investigation, Formal analysis, Data curation. **Xin-Hao Xing:** Writing – review & editing, Writing – original draft, Validation, Investigation, Formal analysis, Data curation. **Ren-Yi Lu:** Investigation, Formal analysis, Data curation. **Meng-Xiao Liu:** Validation, Investigation, Data curation. **Wei-Heng Xu:** Supervision, Resources, Project administration. **Hao-Cheng Zhang:** Writing – review & editing, Validation, Investigation, Funding acquisition. **Qing-Jie Zhao:** Supervision, Project administration, Conceptualization. **Yan Wang:** Writing – review & editing, Supervision, Resources, Project administration, Funding acquisition, Conceptualization.

Declaration of competing interest

The authors declare that they have no known competing financial interests or personal relationships that could have appeared to influence the work reported in this paper.

Acknowledgements

We would like to acknowledge Dr. Ren-Hui Wan at Changzheng Hospital, Second Military Medical University (Naval Medical University) (Shanghai, 200003, China) for his assistance with the CLP procedures.

Appendix A. Supplementary data

Supplementary data to this article can be found online at https://doi.org/10.1016/j.heliyon.2024.e38608.

List of abbreviations:

ANXA3	Annexin A3
AUC	Area Under Curve
CLP	Cecal Ligation and Puncture
CRP	C-reactive Protein
DAB	Diaminobenzidine
GEO	Gene Expression Omnibus
GS	Gene-trait Significance
mHLA-DR	monocytic Human Leukocyte Antigen DR
ME	Module Eigengene
PTX3	Pentraxin-3
PBS	Phosphate Buffer Saline
PCT	Procalcitonin
qSOFA	quick Sequential Organ Failure Assessment
ROC	Receiver Operating Characteristic
SOFA	Sequential Organ Failure Assessment
WGCNA	Weighted Gene Co-expression Network Analysis

References

[1] M. Singer, C.S. Deutschman, C.W. Seymour, M. Shankar-Hari, D. Annane, M. Bauer, et al., The third international consensus definitions for sepsis and septic shock (Sepsis-3), JAMA 315 (8) (2016) 801–810.
[2] K. Reinhart, R. Daniels, N. Kissoon, F.R. Machado, R.D. Schachter, S. Finfer, Recognizing sepsis as a global health priority - a WHO resolution, N. Engl. J. Med. 377 (5) (2017) 414–417.
[3] C. Fleischmann, A. Scherag, N.K.J. Adhikari, C.S. Hartog, T. Tsaganos, P. Schlattmann, et al., Assessment of global incidence and mortality of hospital-treated sepsis. Current estimates and limitations, Am. J. Respir. Crit. Care Med. 193 (3) (2016) 259–272.
[4] M. Bauer, H. Gerlach, T. Vogelmann, F. Preissing, J. Stiefel, D. Adam, Mortality in sepsis and septic shock in Europe, North America and Australia between 2009 and 2019- results from a systematic review and meta-analysis, Crit. Care 24 (1) (2020) 239.
[5] S.Q. Simpson, New sepsis criteria: a change we should not make, Chest 149 (5) (2016) 1117–1118.
[6] S. Lambden, P.F. Laterre, M.M. Levy, B. Francois, The SOFA score-development, utility and challenges of accurate assessment in clinical trials, Crit. Care 23 (1) (2019) 374.
[7] M. Tan, Y. Lu, H. Jiang, L. Zhang, The diagnostic accuracy of procalcitonin and C-reactive protein for sepsis: a systematic review and meta-analysis, J. Cell. Biochem. 120 (4) (2019) 5852–5859.
[8] S.-K. Hung, H.-M. Lan, S.-T. Han, C.-C. Wu, K.-F. Chen, Current evidence and limitation of biomarkers for detecting sepsis and systemic infection, Biomedicines 8 (11) (2020).
[9] P. Langfelder, S. Horvath, WGCNA: an R package for weighted correlation network analysis, BMC Bioinf. 9 (2008) 559.
[10] X. Zhao, L. Zhang, J. Wang, M. Zhang, Z. Song, B. Ni, et al., Identification of key biomarkers and immune infiltration in systemic lupus erythematosus by integrated bioinformatics analysis, J. Transl. Med. 19 (1) (2021) 35.
[11] Q. Wan, J. Tang, Y. Han, D. Wang, Co-expression modules construction by WGCNA and identify potential prognostic markers of uveal melanoma, Exp. Eye Res. 166 (2018) 13–20.
[12] N. Zhang, Y. Liu, C. Yang, X. Li, Review of the predictive value of biomarkers in sepsis mortality, Emerg Med Int 2024 (2024) 2715606.
[13] M. Wang, L. Wang, L. Pu, K. Li, T. Feng, P. Zheng, et al., LncRNAs related key pathways and genes in ischemic stroke by weighted gene co-expression network analysis (WGCNA), Genomics 112 (3) (2020) 2302–2308.
[14] Z. Tian, W. He, J. Tang, X. Liao, Q. Yang, Y. Wu, et al., Identification of important modules and biomarkers in breast cancer based on WGCNA, OncoTargets Ther. 13 (2020) 6805–6817.
[15] D. Rittirsch, M.S. Huber-Lang, M.A. Flierl, P.A. Ward, Immunodesign of experimental sepsis by cecal ligation and puncture, Nat. Protoc. 4 (1) (2009) 31–36.
[16] A. Vega-Pérez, L.H. Villarrubia, C. Godio, A. Gutiérrez-González, L. Feo-Lucas, M. Ferriz, et al., Resident macrophage-dependent immune cell scaffolds drive anti-bacterial defense in the peritoneal cavity, Immunity 54 (11) (2021).
[17] X. Rao, X. Huang, Z. Zhou, X. Lin, An improvement of the 2ˆ(-delta delta CT) method for quantitative real-time polymerase chain reaction data analysis, Biostat Bioinforma Biomath 3 (3) (2013) 71–85.
[18] A. Rasooli, E. Ghafari, H. Saedi, S. Miri, Expression changes of CD177 and MPO as novel biomarkers in lung tissue of CLP model rats, Turk. J. Med. Sci. 48 (6) (2018) 1321.
[19] J. Demaret, F. Venet, J. Plassais, M.-A. Cazalis, H. Vallin, A. Friggeri, et al., Identification of CD177 as the most dysregulated parameter in a microarray study of purified neutrophils from septic shock patients, Immunol. Lett. 178 (2016) 122–130.
[20] M. Toufiq, J. Roelands, M. Alfaki, B. Syed Ahamed Kabeer, M. Saadaoui, A.P. Lakshmanan, et al., Annexin A3 in sepsis: novel perspectives from an exploration of public transcriptome data, Immunology 161 (4) (2020) 291–302.
[21] R. Porte, S. Davoudian, F. Asgari, R. Parente, A. Mantovani, C. Garlanda, et al., The long Pentraxin PTX3 as a humoral innate immunity functional player and biomarker of infections and sepsis, Front. Immunol. 10 (2019) 794.
[22] G. Monneret, F. Venet, Sepsis-induced immune alterations monitoring by flow cytometry as a promising tool for individualized therapy, Cytometry B Clin Cytom 90 (4) (2016) 376–386.
[23] J.D. Faix, Biomarkers of sepsis, Crit. Rev. Clin. Lab Sci. 50 (1) (2013) 23–36.
[24] J.-X. Zhang, W.-H. Xu, X.-H. Xing, L.-L. Chen, Q.-J. Zhao, Y. Wang, ARG1 as a promising biomarker for sepsis diagnosis and prognosis: evidence from WGCNA and PPI network, Hereditas 159 (1) (2022) 27.

[25] H.-x. Lu, C.-c. Ma, D.-l. Wen, G.-s. Chen, F. Zhang, G. Xu, et al., Evaluation and validation of the increased annexin A3 (ANXA3) as a novel biomarker to predict sepsis in critically ill patients, Research Square (2022).
[26] S.E. Moss, R.O. Morgan, The annexins, Genome Biol. 5 (4) (2004) 219.
[27] J. Sopkova, C. Raguenes-Nicol, M. Vincent, A. Chevalier, A. Lewit-Bentley, F. Russo-Marie, et al., Ca(2+) and membrane binding to annexin 3 modulate the structure and dynamics of its N terminus and domain III, Protein Sci. 11 (7) (2002) 1613–1625.
[28] B. Favier-Perron, A. Lewit-Bentley, F. Russo-Marie, The high-resolution crystal structure of human annexin III shows subtle differences with annexin V, Biochemistry 35 (6) (1996) 1740–1744.
[29] Y. Xi, R. Ju, Y. Wang, Roles of Annexin A protein family in autophagy regulation and therapy, Biomed. Pharmacother. 130 (2020) 110591.
[30] H.J. Rhee, G.Y. Kim, J.W. Huh, S.W. Kim, D.S. Na, Annexin I is a stress protein induced by heat, oxidative stress and a sulfhydryl-reactive agent, Eur. J. Biochem. 267 (11) (2000) 3220–3225.
[31] A. Chetcuti, S.H. Margan, P. Russell, S. Mann, D.S. Millar, S.J. Clark, et al., Loss of annexin II heavy and light chains in prostate cancer and its precursors, Cancer Res. 61 (17) (2001) 6331–6334.
[32] W.-Q. Zhao, G.H. Chen, H. Chen, A. Pascale, L. Ravindranath, M.J. Quon, et al., Secretion of Annexin II via activation of insulin receptor and insulin-like growth factor receptor, J. Biol. Chem. 278 (6) (2003) 4205–4215.
[33] C. Bianchi, S. Bombelli, F. Raimondo, B. Torsello, V. Angeloni, S. Ferrero, et al., Primary cell cultures from human renal cortex and renal-cell carcinoma evidence a differential expression of two spliced isoforms of Annexin A3, Am. J. Pathol. 176 (4) (2010) 1660–1670.
[34] R. Huber, R. Berendes, A. Burger, H. Luecke, A. Karshikov, Annexin V-crystal structure and its implications on function, Behring Inst. Mitt. (91) (1992) 107–125.
[35] S. Réty, J. Sopková-de Oliveira Santos, L. Dreyfuss, K. Blondeau, K. Hofbauerová, C. Raguénès-Nicol, et al., The crystal structure of annexin A8 is similar to that of annexin A3, J. Mol. Biol. 345 (5) (2005) 1131–1139.
[36] B. Perron, A. Lewit-Bentley, B. Geny, F. Russo-Marie, Can enzymatic activity, or otherwise, be inferred from structural studies of annexin III? J. Biol. Chem. 272 (17) (1997) 11321–11326.
[37] J.D. Ernst, E. Hoye, R.A. Blackwood, D. Jaye, Purification and characterization of an abundant cytosolic protein from human neutrophils that promotes Ca2(+)-dependent aggregation of isolated specific granules, J. Clin. Investig. 85 (4) (1990) 1065–1071.
[38] V. Le Cabec, I. Maridonneau-Parini, Annexin 3 is associated with cytoplasmic granules in neutrophils and monocytes and translocates to the plasma membrane in activated cells, Biochem. J. 303 (Pt 2) (1994) 481–487.
[39] Z. Zhang, Z. Li, Z. Ma, M. Deng, M. Xing, J. Wu, et al., Annexin A3 as a marker protein for microglia in the central nervous system of rats, Neural Plast. 2021 (2021) 5575090.
[40] E. Abraham, M.P. Glauser, T. Butler, J. Garbino, D. Gelmont, P.F. Laterre, et al., p55 Tumor necrosis factor receptor fusion protein in the treatment of patients with severe sepsis and septic shock. A randomized controlled multicenter trial. Ro 45-2081 Study Group, JAMA 277 (19) (1997) 1531–1538.
[41] E. Abraham, J. Arcaroli, A. Carmody, H. Wang, K.J. Tracey, Cutting edge: HMG-1 as a mediator of acute lung inflammation, J. Immunol. 165 (6) (2000) 2950–2954.
[42] J. Liang, J. Zhang, J. Fan, S. Chen, W. Wu, ANXA3 interference inactivates ERK/ELK1 pathway to mitigate inflammation and apoptosis in sepsis-associated acute lung injury, Mol. Immunol. 167 (2024) 25–33.
[43] Z. Huang, Z. Cheng, X. Deng, Y. Yang, N. Sun, P. Hou, et al., Integrated bioinformatics exploration and preliminary clinical verification for the identification of crucial biomarkers in severe cases of COVID-19, J. Inflamm. Res. 17 (2024) 1561–1576.
[44] L. Liu, Y. Cai, C. Deng, Identification of ANXA3 as a biomarker associated with pyroptosis in ischemic stroke, Eur. J. Med. Res. 28 (1) (2023) 596.
[45] D.-Q. Li, M. Lin, Z. Abdelrahman, High expression of the ANXA3 gene promotes immune infiltration and improves tumor prognosis in ovarian serous carcinoma using bioinformatics analyses, Ann. Transl. Med. 10 (19) (2022) 1055.